

A model of fractional-order diffusion in the glial scar

Dimiter Prodanov* and Jean Delbeke

March 24, 2022

Abstract

Implantation of neuroprosthetic electrodes induces a stereotypical state of neuroinflammation, which is thought to be detrimental for the neurons surrounding the electrode. Mechanisms of this type of neuroinflammation are still not understood well. Recent experimental and theoretical results point out possible role of the diffusion species in this process.

The paper considers a model of anomalous diffusion occurring in the glial scar around a chronic implant in two simple geometries – a separable rectilinear electrode and a cylindrical electrode, which are solvable exactly. We describe a hypothetical extended source of diffusing species and study its concentration profile in steady-state conditions. Diffusion transport is assumed to obey a fractional-order Fick law, which is derived from physically realistic assumptions using a fractional calculus approach. The derived fractional-order distribution morphs into regular order diffusion in the case of integer fractional exponents. The model presented here demonstrates that accumulation of diffusing species can occur and the scar properties (i.e. tortuosity, fractional order, scar thickness) can influence such accumulation. The observed shape of the concentration profile corresponds qualitatively with GFAP profiles reported in the literature. The main difference with respect to the previous studies is the explicit incorporation of the apparatus of fractional calculus without assumption of an ad hoc tortuosity parameter. Intended application of the approach is the study of diffusing substances in the glial scar after implantation of neural prostheses, although the approach can be adapted to other studies of diffusion in biological tissues, for example of biomolecules or small drug molecules.

1 Introduction

Implantation of neuroprosthetic electrodes induces a sustained state of neuroinflammation and scarring, which is thought to be detrimental for the neurons

*Correspondence: Environment, Health and Safety, IMEC vzw, Kapeldreef 75, 3001 Leuven, Belgium; e-mail: Dimiter.Prodanov@imec.be, dimiterpp@gmail.com

surrounding the electrode [18]. Literature demonstrates that in chronic conditions the recording longevity of such electrodes in experimental animals is highly variable (i.e. for wire electrodes - [13], silicon-based electrodes and multi-wire arrays -[38]). Over 100 studies have described stereotypic features of the brain response to microelectrodes that occur irrespective of the type of implant, method of sterilization, species studied, or implantation method [8].

The formation of the glial scar is a complex reactive process involving interactions between several types of cells, notably astrocytes and activated microglia, which are mediated by plethora of bio-active molecules (i.e. cytokins). The reactive *astrocytes* form a dense web of interdigitated processes which over-expresses the Glial Fibrillary Acidic Protein (GFAP) and attach to the implant (see Fig. 1). Thus GFAP is commonly used in neuroprosthetic studies as a marker of neuroninflammation. In parallel, the *microglia* are rapidly activated in a wide area around the lesion site and undergo a profound change in cell shape and phenotype. Concurrent with the glial scar formation, neuronal density within the recording radius of the microelectrodes is reduced, leading to even fewer distinguishable single-unit recordings [5, 37, 10, 1, 31]. During this process the cells change substantially the composition, the morphology and the functional properties of the extracellular matrix. Roitbak and Syková [33] also demonstrate changes of the diffusion path in reactive astrogliosis states and therefore in the extracellular space (ECS) properties.

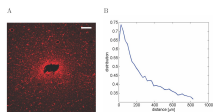


Figure 1: GFAP distribution around an implant site

A – GFAP staining after 6 weeks of implantation in tethered configuration; B – Mean intensity distribution as a function of the distance to the insertion track [30]. The dataset was published previously in [39]. Scale bar – 200 μm .

Several hypotheses for these observations have been put forward. Some authors proposed that formation of *glial scar results in a physical barrier* to diffusing substances, thus creating a toxic environment for the neurons. Others

have proposed that many neurons around the electrodes die shortly after implantation [5, 1]. More recently, McConnell et al. [18] have proposed that the observed loss of signal can also result from the *progressive degeneration of nerve fibers and synapses* due to persistent local chronic inflammation. Ward et al. attribute electrode failure to the traumatic injury resulting from insertion and a long-term foreign body response to the implant [38].

While there are observations supporting each hypothesis there is no agreement as to which is the predominant effect at different time scales (review in [26, 12]). Quantitative histological descriptions of the glial scar may therefore demonstrate these effects more convincingly and provide metrics for more robust safety and biocompatibility assays for neural prostheses.

In this paper we study accumulation of a diffusing species in steady-state conditions, produced as a reaction to the presence of another object, i.e. an implanted electrode. We hypothesize that such conceptual model can describe diffusion phenomena occurring in the extracellular matrix following implantation of flat electrodes, for example Michigan type of silicon probes or cylindrical electrodes, such as microwires.

2 Extended source compartment model

Implanted electrodes have simple cross-section geometries and high aspect ratio with regard to height. In such way, implant geometry can be approximated as consisting of ideal shapes, i.e. an infinite cylinder, a line or a half-plane. This allows for applying a symbolic calculation approach in the modeling of the diffusion problem.

As an idealized situation we will consider semi-infinite medium with **two** spatial compartments: a *source compartment* (S) and a *tissue compartment* (T), (see Fig. 2). To simplify calculation we will assume that the S-compartment will have only constant production of diffusing species but no degradation, while the T-compartment will have only first order degradation but no production.



Figure 2: Model geometry: The extended source model comprises two compartments: source (S) and tissue (T).

The overall solution will be represented by a sum of two terms

$$c(x) = c_s(x) + c_f(x)$$

for the two coupled domains. In the following presentation the term c_s will represent the concentration of the substance in the glial scar, i.e. the S-

compartment. while the second term c_f will represent the concentration in the outer zone – i.e. the T-compartment.

Further, the terms are assumed to be orthogonal, i.e. $c_s(x) = 0$ in the distal compartment $x > L$ whereas $c_f(x) = 0$ in the proximal compartment $x < L$. Since the overall solution is assumed to be continuous the following conditions will have to be imposed on the boundary between domains:

$$\begin{aligned} c_s(x)|_{x=L-} &= c_f(x)|_{x=L+} \\ \frac{\partial c_s}{\partial x}(x)|_{x=L-} &= \frac{\partial c_f}{\partial x}(x)|_{x=L+} \end{aligned}$$

In addition, we also assume natural boundary conditions in steady state – $c(0) = c_0$, $c(\infty) = 0$. Subsequent analysis is performed both in traditional partial differential equation setting and in fractional calculus (i.e. differ-integral) approach as a possible conceptual generalization.

3 Anomalous diffusion in complex media

At present it is well established that the ECS occupies a volume fraction of between 15 and 30% in normal adult brain tissue with a typical value of 20% and that this falls to 5% during global ischemia [36]. Therefore, the diffusion impediment can not be neglected in modeling of biological diffusion. Impeded diffusion can be modeled by two classes of models.

3.1 Regular impeded diffusion

In this framework, the medium imposes only a spatial impediment on the diffusing species and does not change the diffusion law. Nicholson et al [22, 21] consider that the densely packed cells of the brain and their interstitial spaces resemble a porous medium with two phases, an intra- and extracellular phase. Diffusion in the permeable phase of porous media is analogous to the diffusion in the narrow spaces between brain cells, i.e. the extracellular space, ECS.

In accordance, volume transport of species having concentration c is governed by the rescaled reaction-diffusion equation:

$$\frac{\partial c}{\partial t} = \frac{D}{\lambda^2} \nabla^2 c + \frac{s}{\alpha} - \kappa c, \quad \lambda = \sqrt{\frac{D}{D}}$$

where the source term is denoted by s (1/concentration), the clearance term denoted by $k(c) = \kappa c$ is assumed to be first order decay and D is the diffusion coefficient (length²/ time). The following additional parameters are represented respectively by the parameters λ – tortuosity (dimensionless); α – porosity coefficient (dimensionless); κ – clearance speed (1/time).

Unless stated explicitly, we will further use a re-parametrization of the problem preserving the form and interpretation of the equations:

$$\bar{D} = \frac{D}{\lambda^2}, \quad \bar{s} = \frac{s}{\alpha}$$

3.2 Fractional diffusion phenomena

Since the brain extracellular space is a complex medium this transport equation can be regarded only as an *linear approximation*. In accordance, tortuosity can be considered as the linear correction for the anomalous diffusion [21] and [36].

Diffusion in porous media, such as tissues, are characterized by deviation from the usual Fick's diffusion laws. Notably, these processes are characterized by a distribution of waiting times, having heavy tails approximated by an inverse fractional power law, and hence, dependence of the effective diffusion phenomenon on the duration of the measurement. Also the law of the mean squared displacements exhibits deviations from linearity. The resulting behavior can not be described by an ordinary differential equation.

Since the end of the XXth century a different approach to handle deviations from the classical diffusion and hence the anomalous diffusion phenomena has been employed. In this framework the underlying physical process is modeled as a *continuous time random walks* [20], using the mathematical apparatus of fractional calculus [24]. In the fractional calculus approach the transport equation reads

$$\frac{\partial c}{\partial t} = D \nabla \cdot \nabla^\beta c + s - \kappa c$$

where ∇^β denotes the fractional-order Fick's law, i.e. the fractional flux in the system. Interpretation for the symbol of the last operator will be given further in the relevant sections of the paper. This form of the fractional Fick's law naturally implies spatial non-locality and can be derived from rigorous approaches using spatial averaging theorems [19, 40].

4 Linear geometry

4.1 Regular diffusion along the line

In this case we consider the following system:

$$\begin{aligned} \frac{\partial c_s}{\partial t} &= D \frac{\partial^2 c_s}{\partial x^2} - \kappa c_s \\ \frac{\partial c_f}{\partial t} &= D \frac{\partial^2 c_f}{\partial x^2} + s \end{aligned}$$

In steady state the equations have the following general solutions:

$$\begin{aligned} c_s(x) &= -\frac{s x^2}{2D} + k_5 x + k_3 \\ c_f(x) &= k_1 e^{\sqrt{\frac{\kappa}{D}} x} + k_2 e^{-\sqrt{\frac{\kappa}{D}} x} \end{aligned}$$

Then since the solution is limited $k_1 = 0$. After some algebraic transformations we arrive at the following algebraic system to be solved

$$\begin{aligned} -\frac{s L^2}{2D} + k_5 L + k_3 &= k_2 e^{-\sqrt{\frac{\kappa}{D}} L} \\ k_5 - \frac{s L}{D} &= -\frac{k_2 \sqrt{\kappa} e^{-\sqrt{\frac{\kappa}{D}} L}}{\sqrt{D}} \end{aligned}$$

Assuming further parametrization by $k_3 = c(0) = c_0$ we get

$$\begin{aligned} c_s(x) &= -\frac{s}{2D} x^2 + \frac{\sqrt{\kappa} s L^2 + 2s\sqrt{D}L - 2c_0\sqrt{\kappa}D}{2D(\sqrt{\kappa}L + \sqrt{D})} x + c_0, \quad x \in [0, L] \\ c_f(x) &= \frac{s L^2 + 2c_0 D}{2(\sqrt{\kappa} D L + D)} e^{-\sqrt{\frac{\kappa}{D}}(L-x)}, \quad x \geq L \end{aligned}$$

The maximum concentration is attained at

$$x_m = L - \frac{c_0 \frac{\sqrt{\kappa} D}{s} + \sqrt{\frac{\kappa}{D}} \frac{L^2}{2}}{1 + L \sqrt{\frac{\kappa}{D}}}$$

It is easy to check that at $x = 2x_m$ we have $c_s(2x_m) = c_0$.

4.2 Fractional diffusion along the line

The fractional Fick's law in this case reduces to the fractional derivative of a function in the sense of Caputo [3],[4]. This derivative is in turn defined by the differ-integral:

$$\mathbf{D}_a^\beta f(x) = \frac{1}{\Gamma(1-\beta)} \int_a^x \frac{f'(t)}{(x-t)^\beta} dt,$$

where $\Gamma(\cdot)$ is the Euler's gamma function, which for integer number is equal to the factorial $\Gamma(n) = (n-1)!$

The fractional Fick's law is given in this case by

$$j = -D \mathbf{D}_a^\beta c$$

For the convenience of the reader a simple derivation is presented in Appendix A. Combining this equation with a conservation of mass equation for

the concentration of particles leads to the fractional diffusion equation of the type.

$$\frac{\partial c}{\partial t} = D \frac{\partial}{\partial x} \mathbf{D}_0^\beta c + s$$

In the S compartment the equation yields

$$\frac{\partial}{\partial x} \mathbf{D}_0^\beta c_s + \frac{s}{D} = 0,$$

with a solution

$$c_s(x) = \frac{k_5 (1 + \beta) D x^\beta - s x^{\beta+1}}{\Gamma(\beta + 2) D} + c_0$$

For the T compartment since the first derivative of the equation is constrained at the boundary we will reformulate the problem entirely in terms of Caputo derivatives.

$$D \mathbf{D}_0^{1+\beta} c_f - \kappa c_f = 0,$$

The equation can be solved in terms of special functions [17, 16]. The general solution is given by

$$c_f(x) = C_1 E_{1+\beta,1} \left({}^{1+\beta} \sqrt{\frac{\kappa}{D}} x |x|^\beta \right) + C_2 x E_{1+\beta,2} \left({}^{1+\beta} \sqrt{\frac{\kappa}{D}} x |x|^\beta \right)$$

where the $E_{a,b}$ denotes the Mittag-Leffler function (see Appendix B). To avoid unbounded solutions at infinity we pick up constants with opposite signs.

Therefore, finally

$$c_f(x) = C \left(E_{1+\beta,1} \left({}^{1+\beta} \sqrt{\frac{\kappa}{D}} x |x|^\beta \right) - x E_{1+\beta,2} \left({}^{1+\beta} \sqrt{\frac{\kappa}{D}} x |x|^\beta \right) \right)$$

where the constant C can be determined from the boundary or initial conditions.

Since $\frac{\kappa}{D}$ is assumed to be small we will use further the asymptotic expression valid for small values of x to illustrate the relationship to the integer-order solution.

$$c_f(x) \approx k_2 e^{-1+\beta} \sqrt{\frac{\kappa}{D}} \Gamma(\beta) x$$

The resulting system can be solved by subsequent integration using eq. 6 to yield the following algebraic system

$$\frac{k_5 (1 + \beta) D L^\beta - s L^{\beta+1}}{\Gamma(\beta + 2) D} + c_0 = k_2 e^{-\frac{\Gamma(\beta) \kappa^{\frac{1}{\beta+1}} L}{D^{\frac{1}{\beta+1}}}}$$

$$\frac{k_5 \beta D L^{\beta-1} - s L^\beta}{\Gamma(\beta + 1) D} = -\frac{k_2 \Gamma(\beta) \kappa^{\frac{1}{\beta+1}} e^{-\frac{\Gamma(\beta) \kappa^{\frac{1}{\beta+1}} L}{D^{\frac{1}{\beta+1}}}}}{D^{\frac{1}{\beta+1}}}$$

for the first boundary and second boundary condition, respectively. In the resulting system k_2 and k_5 are unknown constants to be determined by the initial and boundary conditions.

Considering further the steady state gives finally for the proximal compartment

$$c_s(x) = \frac{-s x^{1+\beta}}{\Gamma(\beta+2) D} + \frac{L^{1-\beta} \Gamma(\beta) \kappa^{\frac{1}{\beta+1}} (s L^{\beta+1} - c_0 \Gamma(\beta+2) D) + (\beta+1) s D^{\frac{1}{\beta+1}} L}{\Gamma(\beta+2) D \left(\Gamma(\beta) \kappa^{\frac{1}{\beta+1}} L + \beta D^{\frac{1}{\beta+1}} \right)} x^\beta + c_0, \quad x \in [0, L]$$

while for the distal component

$$c_f(x) = \frac{(s L^{\beta+1} + c_0 \beta \Gamma(\beta+2) D)}{\Gamma(\beta+2) D^{\frac{\beta}{\beta+1}} \left(\Gamma(\beta) \kappa^{\frac{1}{\beta+1}} L + \beta D^{\frac{1}{\beta+1}} \right)} e^{-\Gamma(\beta)^{\frac{1}{\beta+1}} \sqrt{\frac{\kappa}{D}} (x-L)}, \quad x \in [L, \infty)$$

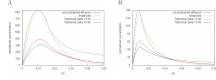


Figure 3: Influence of scar thickness on the steady-state concentration of diffusing species in planar geometry

The *y-axis* shows normalized concentration of species with regards to source flux intensity $\frac{c}{s}$; for simplicity also $c_0 = 0$ was assumed. Notice the slow decay of the fractional-order solution compared to the linearized case. A : L = 150 um, B: L= 50 um.

5 Cylindrical geometry

5.1 Regular cylindrical diffusion

In the case of implanted wire electrodes, we will assume cylindrical symmetry of the problem. The the Laplacian operator can be represented as

$$\nabla^2 c = \frac{1}{r} \frac{\partial}{\partial r} \left(r \frac{\partial c}{\partial r} \right) + \frac{1}{r^2} \frac{\partial^2 c}{\partial \phi^2} + \frac{\partial^2 c}{\partial z^2}$$

We will look only for solutions that are cylindrically and axially symmetric that is $\frac{\partial c}{\partial \phi} = 0$ and $\frac{\partial c}{\partial z} = 0$.

Therefore, we have to consider the following system:

$$\begin{aligned} c(x) &= c_s(x) + c_f(x) \\ \frac{\partial c_s}{\partial t} &= D \frac{1}{r} \frac{\partial}{\partial r} \left(r \frac{\partial c_s}{\partial r} \right) + s \\ \frac{\partial c_f}{\partial t} &= D \frac{1}{r} \frac{\partial}{\partial r} \left(r \frac{\partial c_f}{\partial r} \right) - \kappa c_f \end{aligned}$$

The solution will be presented as a sum of two terms for the two coupled domains where we also impose continuity conditions at the border:

$$\begin{aligned} c_s(r)|_{r=L-} &= c_f(r)|_{r=L+} \\ \frac{\partial c_s}{\partial r}(r)|_{r=L-} &= \frac{\partial c_f}{\partial r}(r)|_{r=L+} \end{aligned}$$

In addition we assume also a natural boundary conditions in steady state:

$$c(0) = c_0, \quad c(\infty) = 0$$

In steady state the equations transform to the following independent system

$$\begin{aligned} D \frac{1}{r} \frac{\partial}{\partial r} \left(r \frac{\partial c_s}{\partial r} \right) + s &= 0, \quad 0 \leq r \leq L \\ D \frac{1}{r} \frac{\partial}{\partial r} \left(r \frac{\partial c_f}{\partial r} \right) - \kappa c_f &= 0, \quad r \geq L \end{aligned}$$

Compartment S The general solution is given by

$$c_s(r) = c_1 - \frac{r^2 s}{4D} - c_2 \log(r)$$

From the finiteness of the solution at the left boundary it follows that $c_2 = 0$ and

$$c_s(r) = c_0 - \frac{s}{4D} r^2 \tag{1}$$

Compartment T The equation can be transformed in the form

$$\frac{\partial}{\partial r} \left(r \frac{\partial}{\partial r} c_f(qr) \right) - q^2 r c_f(qr) = 0$$

with

$$q = \sqrt{\frac{\kappa}{D}},$$

which corresponds to the modified Bessel equation [27] by the ansatz $q^2 c_f(qr) = y(r)$. Notably,

$$r \frac{\partial^2 y}{\partial r^2} + \frac{\partial y}{\partial r} - r y = 0$$

The general solution of this equation is given in terms of the *modified Bessel functions* of the first and second kind, notably :

$$c_f(r) = c_1 K_0(qr) + c_2 I_0(qr)$$

Since $I_0(r)$ diverges at infinity the only acceptable solution is

$$c_f(r) = c_1 K_0(qr)$$

Applying the continuity conditions results in the system

$$\begin{aligned} c_0 - \frac{sL^2}{4D} &= c_1 K_0 \left(\sqrt{\frac{D}{\kappa}} L \right) \\ -\frac{sL}{2D} &= -c_1 K_1 \left(\sqrt{\frac{D}{\kappa}} L \right) \sqrt{\frac{D}{\kappa}} \end{aligned}$$

The system can be solved to yield:

$$\begin{aligned} c_s(r) &= \frac{s(L^2 - r^2)}{4D} + \frac{K_0 \left(\sqrt{\frac{\kappa}{D}} L \right) sL}{K_1 \left(\sqrt{\frac{\kappa}{D}} L \right) \sqrt{\kappa D}}, \quad r \in [0, L] \\ c_f(r) &= \frac{K_0 \left(\sqrt{\frac{\kappa}{D}} r \right) sL}{K_1 \left(\sqrt{\frac{\kappa}{D}} L \right) \sqrt{D\kappa}}, \quad r > L \end{aligned}$$

From the explicit form of solution it can be seen that the value of the concentration at the origin is completely fixed by the geometry of the problem.

5.2 Fractional cylindrical diffusion

Generalization to the 2D case is a considerably more difficult problem. Following the derivation of Meerschaert [19] we define the fractional Fick's law of fractional order $\beta < 1$ as

$$\nabla^\beta = \mathbb{J}^{1-\beta} \nabla$$

where \mathbb{J}^β denotes the vector fractional integral operator.

$$\frac{\partial c}{\partial t} = D \nabla \cdot \nabla^\beta c + s - \kappa c$$

Compartment S Following the derivation of Meerschaert [19] we define the fractional Fick's law. Therefore, in steady state we have

$$D \nabla \cdot \nabla^\beta c_s + s = 0$$

The equation can be solved by Laplace's transform method to yield

$$c_s(r) = c_0 - \frac{r^{\beta+1} s}{D(1+\beta)\Gamma(\beta+2)} + \frac{c_1 r^{\beta-1} s}{D(1-\beta)\Gamma(\beta)}$$

Similar considerations about the boundedness of the solution at $r = 0$ require that $c_1 = 0$.

$$c_s(r) = c_0 - \frac{r^{\beta+1} s}{D(1+\beta)\Gamma(\beta+2)} \quad (2)$$

Compartment T In steady state conditions we have

$$D \nabla \cdot \nabla^\beta c_f - \kappa c_f = 0$$

The Laplace transform method can be also applied in this case, although no explicit solution can be identified (see Appendix C.2). Nevertheless, for completeness of the presentation a similar procedure is applied. This is equivalent to the assumption that the fractional exponent equals two in the T domain.

Applying the continuity conditions results in

$$\begin{aligned} c_0 - \frac{L^{\beta+1} s}{(1+\beta)D\Gamma(\beta+2)} &= c_1 K_0 \left(\sqrt{\frac{D}{\kappa}} L \right) \\ -\frac{s L^\beta}{(1+\beta)D\Gamma(\beta+1)} &= -c_1 K_1 \left(\sqrt{\frac{D}{\kappa}} L \right) \sqrt{\frac{D}{\kappa}} \end{aligned}$$

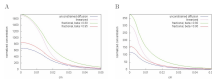


Figure 4: Influence of scar thickness on the steady-state distribution of diffusing species in cylindrical geometry

The *y-axis* shows normalized concentration of species with regards to source flux intensity s . A : $L = 150$ um, B: $L = 50$ um.

6 Analysis of the boundary conditions in the case of a thick electrode

6.1 Vanishing flow

Let's assume that the electrode is thick, with a finite radius ρ . This case is known as the standard Neumann boundary condition

$$\left. \frac{\partial c_s(r)}{\partial r} \right|_{r=\rho} = 0$$

Linear geometry In the case of tight contact between the tissue and the electrode one can assume as well vanishing of the flux at the boundary of the electrode. In this case we will have

$$\frac{\sqrt{k} (s L^2 - 2 c_0 D) + 2 s \sqrt{D} L}{2 \sqrt{k} D L + 2 D^{\frac{3}{2}}} - \frac{\rho s}{D} = 0$$

which gives immediately for the concentration at the boundary

$$c_s(\rho) = \frac{s (L - \rho) (\sqrt{k} L + 2 \sqrt{D} - \sqrt{k} \rho)}{2 \sqrt{k} D}$$

resulting in

$$c_s(x) = \frac{s (L - x) (L + x - 2 \rho)}{2 D} + \frac{s (L - \rho)}{\sqrt{k} \sqrt{D}}$$

The maximum of the last expression is attained at $x = \rho$.

Cylindrical geometry The general solution for the S-compartment is given by

$$c_s(r) = c_1 - \frac{r^2 s}{4D} - c_2 \log(r)$$

After some algebraic manipulations the solution can be simplified to

$$c_s(r) = \frac{\log\left(\frac{r^2}{\rho^2}\right) \rho^2 s}{4D} + \frac{(\rho^2 - r^2) s}{4D} + c_0$$

It can be shown that in the limit $\rho \rightarrow 0$ we can recover

$$c_s(r) = c_0 - \frac{s}{4D} r^2$$

In the case of fractional diffusion after some algebra we can obtain

$$c_s(r) = c_0 - \frac{2 \rho^{\beta+1} s}{(\beta^2 - 1) \Gamma(\beta + 2) D} + \frac{r^{\beta-1} \rho^2 s}{(\beta - 1) \Gamma(\beta + 2) D} - \frac{r^{\beta+1} s}{(\beta + 1) \Gamma(\beta + 2) D}$$

which again for $\rho \rightarrow 0$ and $\beta \rightarrow 1$ reduces to Eq. 1.

6.2 Non-vanishing flow

Let's denote by z the value of the flow attained at the electrode boundary. In this case we have to consider the condition

$$\left. \frac{\partial c_s(r)}{\partial r} \right|_{r=\rho} = z$$

Linear geometry In this case we have the condition

$$\frac{\sqrt{k} (sL^2 - 2k_3 D) + 2s\sqrt{D}L}{2\sqrt{k}DL + 2D^{\frac{3}{2}}} - \frac{\rho s}{D} = z$$

After some algebra we arrive at:

$$c_s(x) = \sqrt{k}D^{\frac{3}{2}}(sL - zD - \rho s) + \frac{(L-x)(sL - 2zD + sx - 2\rho s)}{2D}$$

The position of the peak is attained by solving the equation

$$\frac{s(L-x)}{2D} - \frac{sL - 2zD + sx - 2\rho s}{2D} = 0$$

which gives the unique value

$$x_m = \frac{zD}{s} + \rho$$

Cylindrical geometry In this case we have the condition

$$-\frac{\rho s}{2D} - \frac{c_2}{\rho} = z$$

and after some algebraic manipulations

$$c_s(r) = \frac{\left(\left(\log\left(\frac{r^2}{\rho^2}\right) + 1 \right) \rho^2 - r^2 \right) s}{4D} + \log\left(\frac{r}{\rho}\right) \rho z + c_0$$

It can be shown that in limit $\rho \rightarrow 0$ we can recover

$$c_s(r) = c_0 - \frac{s}{4D}r^2$$

The position of the peak is attained by solving the equation

$$\frac{2\rho zD + \rho^2 s}{2rD} - \frac{rs}{2D} = 0$$

which gives the physically meaningful value of

$$r_m = \sqrt{\rho} \sqrt{\frac{2zD}{s}} + \rho$$

From this analysis it is apparent that the peak position is influenced by the direction of the flux.

7 Numerical analysis

Some numerical results are demonstrated in Fig. 3 using literature values of parameters for rat neocortex, [21].

Available experimental data show that a typical value for small molecules for λ in the nervous system is about 1.6, which implies that \bar{D} is some 2.6 times smaller than D . For macromolecules λ is increased, in part because of more frequent interaction with the walls of the narrow channels through the ECS [23]. Numerical values used in the calculation are as follows: $D = 1.10^{-6} \text{cm}^2 \text{s}^{-1}$ for proteins, $\lambda = 2.5$ (NGF) and $\alpha = 0.21$; uptake $k = 1.10^{-4}$ (NGF). Magin et al. [15] measure experimentally the fractional order of 1.95 using diffusion MRI. This corresponds to the value $\beta = 0.95$ in our parametrization.

All cases use the same values of porosity. The glial scar thickness was taken as the range $L = 50 - 150 \mu\text{m}$. For the unconstrained diffusion case no correction for λ is given. The linearized case corresponds to the approach of Nicholson and Sykova [21, 36]. In the fractional cases no tortuosity correction is applied but only the fractional order β is varied. Results are plotted in Figs. 3 and 4.

8 Discussion

8.1 Diffusion around brain implants

Presented results show that in steady-state conditions substances, which are produced presumably in the glial scar could accumulate and produce characteristic profiles, matching qualitatively empirically observed GFAP and microglial profiles published in available experimental literature. More specifically, shapes of the concentration profiles correspond qualitatively with the GFAP profiles, for example [44, 18, 42, 41, 29, 28, 35], and the blood vessel area distribution [6] reported in literature. In all of these studies implanted probes had planar geometry, therefore reported GFAP profiles can be discussed under the assumptions of the presented model. Presented model can be extrapolated to separable 3D geometries as well considering presence of planar symmetries. The shape of the cylindrical distribution corresponds also to studies employing cylindrical or wire electrodes [32, 10]. Presented approach, therefore, provides means for approximation of such profiles and estimation of geometrical parameters related to the problem, such as the scar thickness and the intensity of the source. In some cases the fractional exponent can supplement the so-far used linearized parameters, such as tortuosity, if such estimates are not available.

Our model demonstrates that ex-centric accumulation of diffusing species can occur and the scar geometry (i.e. tortuosity, fractional order, scar thickness) can influence such accumulation. From the analysis of the boundary condition we can conclude that the insulation of the electrode with regard to the boundary (i.e. presence or absence of lateral flux) determines the shape of the observed profile in both studied geometries. We can therefore speculate, that all studies exhibiting profiles with ex-centric accumulation actually had somehow loose

contact between the implant and the brain tissue, possibly due to micromotion. To further verify that, however, additional efforts in mechanical modeling of devices are necessary.

Recently [35] modeled numerically diffusion around implants in order to design a diffusion sink placed at the device surface that would retain pro-inflammatory cytokines for sufficient time to passively antagonize their impact on the foreign body response. Such setting would correspond to a negative flux condition in our model and it can indeed be shown that this will result in reduction of the gradient. Authors used no-flux boundary conditions and presented results, which qualitatively correspond to the analysis presented here. On the other hand, reported experimental results demonstrate deviations from the numerical model, which can be interpreted well using our model.

8.2 Impeded diffusion phenomena

Anomalous diffusion problems naturally arise in the setting of complex biological environment. Modeling of diffusion in different complex media could provide further understanding in a variety of experimental conditions. Impeded or anomalous diffusion in the brain is already a well established phenomenon [36]. Sykova and Nicholson [36] list several factors that determine diffusion impediments: i) an increase in geometric path length; ii) transient trapping of molecules in dead-space microdomains; iii) an increased interstitial viscous drag on migrating molecules; iv) transient binding to membrane-attached or extracellular matrix-attached receptors; and v) nonspecific interaction with fixed opposite charges. All five factors can be thought of as introducing a delay into the passage of a molecule in brain tissue relative to that in a free medium. Therefore, this complex medium can be conceptually modeled as the presence of two phases – one permeable and one impermeable, which impedes undergoing diffusion.

Fractional diffusion models have been employed in hydrology describing well slow diffusion [19] in protein diffusion in the plasma membrane [11, 9]. The spatial complexity of a medium can impose geometrical constraints on transport processes on all length scales that can fundamentally alter the laws of standard diffusion [20]. Specifically fractional order diffusion models have been employed to model water diffusion in the brain [14].

Fractional models can provide new insights on mesoscopic aspects of the studied phenomena. For example, space fractional models have been used to describe cardiac cell conduction [2], and diffusion phenomena in fixed tissue samples [15].

ECS of the brain comprises the matrix that resides outside the neurons and glia cells, most importantly the interstitial space between neighboring cells. The ECS is a reservoir for ions involved in electrical activity, a communication channel for chemical messengers and a conduit for drug delivery. A quantitative description of extracellular diffusion is important whenever the transport of neurotransmitters, neuromodulators, and therapeutics in the brain ECS is considered. Diffusion-mediated transport of biomolecules substances is hindered

by the ECS structure but the microscopic basis of this hindrance is not fully understood [7]. Evidence for anomalous diffusion in the brain has been found in the rat cerebellum [43], which provides support also for employing fractional models in the continuous approximation limit. Most probably, dead space microdomains can be the cause of such anomalous diffusion [34].

The magnitude of the exponent β can be used as a metrics for the departure from linearity. Since decrease of β will result in behavior approximating advection flow, this can used to reason about state where such flows can be enhance, for example in the case of the leaky blood-brain barrier or in conditions with increased local blood flow.

Acknowledgments

The work has been supported in part by a grant from Research Fund - Flanders (FWO), contract number 0880.212.840.

A Derivation of the fractional-order Fick law

The Riemann-Liouville fractional integral (or differ-integral) defines a weighted average of the function over the interval $[a, x]$ using a power law weighting function.

The Riemann-Liouville differintegral of order $\beta \geq 0$ is defined [24] as

$${}_a\mathbf{I}_x^\beta f(x) = \frac{1}{\Gamma(\beta)} \int_a^x f(t) (x-t)^{\beta-1} dt .$$

The non-local fractional derivative of a function in the sense of Riemann-Liouville is defined in terms of the fractional integral as

$${}_{RL}\mathbf{D}_a^{n+\beta} f(x) = \left(\frac{d}{dx} \right)^n {}_a\mathbf{I}_x^{n-\beta} f(x) \quad (3)$$

which is usually specialized for $n = 1$ in an explicit form by

$${}_{RL}\mathbf{D}_a^\beta f(x) = \frac{1}{\Gamma(1-\beta)} \frac{d}{dx} \int_a^x \frac{f(t)}{(x-t)^\beta} dt .$$

The non-local fractional derivative of a function (in the sense of Caputo) of a function is defined [3],[4] as

$$\mathbf{D}_a^\beta f(x) = {}_a\mathbf{I}_x^{n-\beta} f^{(n)}(x) . \quad (4)$$

or using expanded notation for $n = 1$

$$\mathbf{D}_a^\beta f(x) = \frac{1}{\Gamma(1-\beta)} \int_a^x \frac{f'(t)}{(x-t)^\beta} dt ,$$

where $\Gamma(\cdot)$ is the Euler's function, which for integer number is equal to the factorial $\Gamma(n) = (n - 1)!$.

Both definitions coincide for problems where the function and its first n derivatives vanish at the lower limit of integration, i.e. when $f(a) = 0, \dots, f^{(n)}(a) = 0$. Caputo's definition is better suited for problems where the function and its derivatives do not vanish at this limit, because in this case it is given as kind of regularization of the Riemann-Liouville differintegral to avoid divergences.

Caputo's derivative is a left inverse of the fractional integral:

$$\mathbf{D}_a^\beta \circ {}_a\mathbf{I}_x^\beta f = f(x), \quad (5)$$

while the fractional integral is a conditional inverse of Caputo's derivative:

$${}_a\mathbf{I}_x^\beta \circ \mathbf{D}_a^\beta f = f(x) - f(a^+) \quad (6)$$

in the case when $\mathbf{D}_a^\beta f \neq 0$. This allows one to solve simple fractional systems, such as the fractional diffusion equation in the example.

Fractional Fick's law for an exponent $\beta > 0$ can be derived under the assumption that the transport is given by a wighted fractional average of the differential of concentrations in the domain $[a, x]$. To avoid unphysical divergence at the borders of the domain, which are of interest in our problem we further regularize by subtracting the boundary concentration $c(a)$:

$$dJ_\beta = dx \frac{1}{\Gamma(\beta)} \frac{d}{dx} \int_a^x (c(t) - c(a)) (x - t)^{\beta-1} dt .$$

One can recognize this expression as the usual definition of the Riemann-Liouville fractional derivative. The integral can be evaluated partially assuming as usual existence of the derivative of the concentration $c'(t)$. Then applying integration by parts we get

$$\begin{aligned} & \frac{1}{\Gamma(1 + \beta)} \int_a^x (c(t) - c(a)) d(x - t)^\beta = \\ & \frac{1}{\Gamma(1 + \beta)} (c(t) - c(a)) (x - t)^\beta \Big|_a^x - \frac{1}{\Gamma(1 + \beta)} \int_a^x c'(t) (x - t)^\beta dt = \\ & \qquad \qquad \qquad - \frac{1}{\Gamma(1 + \beta)} \int_a^x c'(t) (x - t)^\beta dt \end{aligned}$$

where we notice that the first term evaluates to zero.

Differentiating the last integral by x gives

$$\begin{aligned} dJ_\beta &= -dx \frac{1}{\Gamma(1 + \beta)} \frac{d}{dx} \int_a^x c'(t) (x - t)^\beta dt = \\ & -dx \frac{\beta}{\Gamma(1 + \beta)} \int_a^x c'(t) (x - t)^{\beta-1} dt = -dx \frac{1}{\Gamma(\beta)} \int_a^x c'(t) (x - t)^{\beta-1} . \end{aligned}$$

However, the last expression can be recognized as $\mathbf{D}_a^{1-\beta} c$. Therefore,

$$j = \frac{dJ_\beta}{dx} = -\mathbf{D}_a^{1-\beta} c \quad (7)$$

B Mittag-Leffler functions

During the last decades fractional calculus has been widely applied in many scientific areas ranging from mathematics and physics, up to biology, engineering, and earth sciences. The Mittag-Leffler functions play an important role in fractional calculus since many solutions of fractional differ-integrals can be expressed in terms of Mittag-Leffler functions.

The one parameter ML function is a generalization of the exponential function:

$$E_\alpha(t) = \sum_{k=0}^{\infty} \frac{t^k}{\Gamma(\alpha k + 1)}, \alpha > 0 \quad (8)$$

The two parameter ML function is an additional generalization in the sense

$$E_{\alpha,\beta}(t) = \sum_{k=0}^{\infty} \frac{t^k}{\Gamma(\alpha k + \beta)}, \alpha > 0 \quad (9)$$

A particular form of the one parameter ML function studied by F. Mainardi is

$$e_\alpha(t) = E_\alpha(-t^\alpha)$$

The following result can be stated

$$\mathbf{D}_0^\alpha e_\alpha(b t) = b e_\alpha(b t).$$

It is common to point out that the function $e(t)$ matches for $t \approx 0$ a stretched whereas as $t \rightarrow \infty$ with a negative power law. The short time approximation is derived from the power series representation as follows [16]

$$e_\alpha(t) \sim \exp\left(-\frac{t^\alpha}{\Gamma(1+\alpha)}\right), \quad t \rightarrow 0$$

$$e_\alpha(t) \sim \frac{1}{1 + \Gamma(1-\alpha)t^\alpha}, \quad t \rightarrow \infty$$

For intermediate ranges, the following approximations can give acceptable results for $\alpha \approx 1$

$$e_\alpha(t) \approx \frac{e^{-\Gamma(1+\alpha)t^\alpha} + \frac{\Gamma(1+\alpha)}{1+\Gamma(1-\alpha)t^\alpha}}{1 + \frac{\Gamma(1+\alpha)}{1+\Gamma(1-\alpha)t^\alpha}}$$

and

$$e_\alpha(t) \approx \frac{e^{-\Gamma(a)x} + \frac{1}{1+\frac{x}{a}}}{1 + \frac{1}{1+\frac{x}{a}}}$$

C Laplace transform method for solving fractional differential equations

Since we are dealing with a problem in the positive half-plane the Laplace integral transform method can be applied for solving all presented differential equations. We further outline the main steps of the solution procedures.

C.1 Integer order case

Considering the flux conditions the following equation can be stated for the Green's function:

$$\frac{D}{r} \frac{\partial f}{\partial r} + D \frac{\partial^2 f}{\partial r^2} + s = -c_1 \frac{\delta(r)}{r}$$

the Laplace transform of the equation is as follows

$$-D p^2 \frac{\partial F}{\partial p} - D p F + \frac{s}{p^2} = -c_1$$

which can be solved to give

$$F(p) = -\frac{s}{2p^3 D} + c_1 \frac{\log(p)}{p D} + \frac{c}{p}$$

the inverse Laplace transform gives

$$f(r) = -\frac{r^2 s}{4 D} - \frac{c_1 \log(r)}{D} + c$$

C.2 Fractional order case

The fractional diffusion equation can be transformed in the Laplace domain using the properties of the Laplace transform for the Caputo fractional derivative. Briefly, if $\mathcal{L} : f(t) \mapsto F(s)$ denotes the Laplace transform then the Caputo derivative is transformed according to the following rule:

$$\mathcal{L} : \mathbf{D}_0^{n+\beta} f(x) \mapsto s^{\beta-1} \left(s^{n+1} F(s) - \sum_{k=0}^n f^{(k)}(0) s^{n-k} \right)$$

S-compartment The Green's function equation in the spatial domain reads

$$\frac{D}{r} \frac{\partial}{\partial r} r \mathbf{D}_a^\beta f(r) + s = -c_1 \frac{\delta(r)}{r}$$

The Laplace transform gives the ordinary differential equation

$$-D s^{\beta+1} \frac{\partial F}{\partial p} - D p^\beta F + \frac{s}{p^2} = -c_1$$

with a solution

$$F(p) = \frac{c_0}{p} - \frac{s p^{-\beta-2}}{D(\beta+1)} - \frac{c_1 s}{D(\beta-1) p^\beta}$$

Which gives

$$f(r) = c_0 - \frac{s r^{\beta+1}}{D(\beta+1) \Gamma(\beta+2)} - \frac{c_1 s r^{\beta-1}}{D(1-\beta) \Gamma(\beta)}$$

T-compartment The Fractional diffusion equation for the Green's function reads

$$\frac{D}{r} \frac{\partial}{\partial r} r \mathbf{D}_a^\beta f(r) - \kappa f(r) = -c_2 \frac{\delta(r)}{r}$$

which can be expanded into

$$rD \mathbf{D}_a^{1+\beta} f(r) + D \mathbf{D}_a^\beta f(r) - \kappa r f(r) = -c_2 \delta(r)$$

This equation in turn can be transformed into the Laplace domain as

$$(\kappa - D p^{\beta+1}) \frac{\partial F}{\partial p} - D p^\beta F = -c_2$$

The last equation can be solved in special functions, notably

$$F(p) = c_2 \frac{1}{(D p^{1+\beta} - \kappa)^{\frac{1}{\beta+1}}} + c_1 \frac{p}{k^{\beta/(1+\beta)} (D p^{1+\beta} - \kappa)^{\frac{1}{\beta+1}}} {}_2F_1 \left(\frac{1}{\beta+1}, \frac{\beta}{\beta+1}; \frac{1}{\beta+1} + 1; \frac{D}{\kappa} p^{\beta+1} \right)$$

where ${}_2F_1(a, b; c; z)$ is the Gauss hypergeometric function [25, ch. 15]. Unfortunately, the inverse Laplace transform of the general solution is not known. However, as a verification of so-obtained solution for the case $\beta = D = \kappa = 1$ we can obtain [25, ch. 15]:

$$F(p) = c_2 \frac{1}{\sqrt{p^2 - 1}} + c_1 \frac{\text{acosh}(p)}{\sqrt{p^2 - 1}} .$$

Transforming back to the spatial domain this gives a general solution in terms of modified Bessel functions:

$$f(r) = c_2 I_0(r) + c_1 K_0(r) .$$

References

- [1] Roy Biran, David C Martin, and Patrick A Tresco. Neuronal cell loss accompanies the brain tissue response to chronically implanted silicon microelectrode arrays. *Exp Neurol*, 195(1):115–126, Sep 2005.
- [2] A. Bueno-Orovio, D. Kay, V. Grau, B. Rodriguez, and K. Burrage. Fractional diffusion models of cardiac electrical propagation: role of structural heterogeneity in dispersion of repolarization. *Journal of The Royal Society Interface*, 11(97):20140352, 2014.
- [3] M. Caputo. Linear models of dissipation whose Q is almost frequency independent ii. *Geophys J R Ast Soc*, 13(529):529–539, 1967.

- [4] M. Caputo and F. Mainardi. Linear models of dissipation in anelastic solids. *Rivista del Nuovo Cimento*, 1:161 – 198, 1971.
- [5] D. J. Edell, V. V. Toi, V. M. McNeil, and L. D. Clark. Factors influencing the biocompatibility of insertable silicon microshafts in cerebral cortex. *IEEE Trans Biomed Eng*, 39(6):635–643, Jun 1992.
- [6] L. Grand, L. Wittner, S. Herwik, E. Göthelid, P. Ruther, S. Oscarsson, H. Neves, B. Dombóvári, R. Csercsa, G. Karmos, and I. Ulbert. Short and long term biocompatibility of neuroprobes silicon probes. *J Neurosci Methods*, 189(2):216–229, Jun 2010.
- [7] Sabina Hrabetov, Jan Hrabec, and Charles Nicholson. Dead-space microdomains hinder extracellular diffusion in rat neocortex during ischemia. *J Neurosci*, 23(23):8351–8359, Sep 2003.
- [8] Mehdi Jorfi, John L. Skousen, Christoph Weder, and Jeffrey R. Capadona. Progress towards biocompatible intracortical microelectrodes for neural interfacing applications. *J Neural Eng*, 12(1):011001, Feb 2015.
- [9] Atefeh Khoshnood and Mir Abbas Jalali. Anomalous diffusion of proteins in sheared lipid membranes. *Phys Rev E Stat Nonlin Soft Matter Phys*, 88(3):032705, 2013.
- [10] Young-Tae Kim, Robert W Hitchcock, Michael J Bridge, and Patrick A Tresco. Chronic response of adult rat brain tissue to implants anchored to the skull. *Biomaterials*, 25(12):2229–2237, May 2004.
- [11] S. C. Kou and X Sunney Xie. Generalized langevin equation with fractional gaussian noise: subdiffusion within a single protein molecule. *Phys Rev Lett*, 93(18):180603, 2004.
- [12] Jennie B Leach, Anil Kumar H Achyuta, and Shashi K Murthy. Bridging the divide between neuroprosthetic design, tissue engineering and neurobiology. *Front Neuroeng*, 2:18, 2010.
- [13] X. Liu, D. B. McCreery, R. R. Carter, L. A. Bullara, T. G. Yuen, and W. F. Agnew. Stability of the interface between neural tissue and chronically implanted intracortical microelectrodes. *IEEE Trans Rehabil Eng*, 7(3):315–326, Sep 1999.
- [14] Richard L. Magin, Osama Abdullah, Dumitru Baleanu, and Xiaohong Joe Zhou. Anomalous diffusion expressed through fractional order differential operators in the bloch-torrey equation. *J Magn Reson*, 190(2):255–270, Feb 2008.
- [15] Richard L. Magin, Carson Ingo, Luis Colon-Perez, William Triplett, and Thomas H. Mareci. Characterization of anomalous diffusion in porous biological tissues using fractional order derivatives and entropy. *Microporous Mesoporous Mater*, 178:39–43, Sep 2013.

- [16] F. Mainardi. *Fractals and Fractional Calculus in Continuum Mechanics*, chapter Fractional Calculus: Some Basic Problems in Continuum and Statistical Mechanics, pages 291 – 348. Springer, Wien and New York, 1997.
- [17] F. Mainardi, Y. Luchko, and G. Pagnini. The fundamental solution of the space-time fractional diffusion equation. *Fract. Calc. Appl. Anal.*, 4(2):153 – 192, 2001.
- [18] George C McConnell, Howard D Rees, Allan I Levey, Claire-Anne Gutekunst, Robert E Gross, and Ravi V Bellamkonda. Implanted neural electrodes cause chronic, local inflammation that is correlated with local neurodegeneration. *J Neural Eng*, 6(5):056003, Oct 2009.
- [19] Mark M. Meerschaert, Jeff Mortensen, and Stephen W. Wheatcraft. Fractional vector calculus for fractional advection-dispersion. *Physica A: Statistical Mechanics and its Applications*, 367:181–90, 2006.
- [20] Ralf Metzler and Joseph Klafter. The restaurant at the end of the random walk: recent developments in the description of anomalous transport by fractional dynamics. *Journal of Physics A: Mathematical and General*, 37(31):R161, 2004.
- [21] C. Nicholson. Diffusion and related transport properties in brain tissue. *Rep Prog Phys*, 64:815 – 884, 2001.
- [22] C. Nicholson, K. C. Chen, S. Hrabětová, and L. Tao. Diffusion of molecules in brain extracellular space: theory and experiment. *Prog Brain Res*, 125:129–154, 2000.
- [23] Charles Nicholson, Padideh Kamali-Zare, and Lian Tao. Brain extracellular space as a diffusion barrier. *Comput Vis Sci*, 14(7):309–325, Oct 2011.
- [24] K.B. Oldham and J.S. Spanier. *The Fractional Calculus: Theory and Applications of Differentiation and Integration to Arbitrary Order*. Academic Press, New York, 1974.
- [25] F. W. J. Olver, D. W. Lozier, R. F. Boisvert, and C. W. Clark, editors. *NIST Handbook of Mathematical Functions*. Cambridge University Press, New York, NY, 2010. Print companion to [?].
- [26] V. S. Polikov, P. A. Tresco, and W. M. Reichert. Response of brain tissue to chronically implanted neural electrodes. *J Neurosci Methods*, 148(1):1–18, Oct 2005.
- [27] A. D. Polyanin and V. F. Zaitsev. *Handbook of Exact Solutions for Ordinary Differential Equations*. Chapman & Hall/CRC, Boca Raton., 2 edition, 2003.

- [28] Kelsey A. Potter, Amy C. Buck, Wade K. Self, Megan E. Callanan, Smrithi Sunil, and Jeffrey R. Capadona. The effect of resveratrol on neurodegeneration and blood brain barrier stability surrounding intracortical microelectrodes. *Biomaterials*, 34(29):7001–7015, Sep 2013.
- [29] Kelsey A. Potter, Amy C. Buck, Wade K. Self, and Jeffrey R. Capadona. Stab injury and device implantation within the brain results in inversely multiphasic neuroinflammatory and neurodegenerative responses. *J Neural Eng*, 9(4):046020, Aug 2012.
- [30] D. Prodanov and K. Verstreken. *Molecular Imaging*, chapter Automated Segmentation and Morphometry of Cell and Tissue Structures. Selected Algorithms in ImageJ, pages 183 – 208. Molecular Imaging. InTech, Rijeka, 2012.
- [31] Erin K Purcell, David E Thompson, Kip A Ludwig, and Daryl R Kipke. Flavopiridol reduces the impedance of neural prostheses in vivo without affecting recording quality. *J Neurosci Methods*, 183(2):149–157, Oct 2009.
- [32] Li Rao, Haihan Zhou, Tao Li, Chengyan Li, and Yanwen Y Duan. Polyethylene glycol-containing polyurethane hydrogel coatings for improving the biocompatibility of neural electrodes. *Acta Biomater*, Mar 2012.
- [33] T. Roitbak and E. Syková. Diffusion barriers evoked in the rat cortex by reactive astrogliosis. *Glia*, 28(1):40–48, Oct 1999.
- [34] Ang Doma Sherpa, Paula van de Nes, Fanrong Xiao, Jeremy Weedon, and Sabina Hrabetova. Gliotoxin-induced swelling of astrocytes hinders diffusion in brain extracellular space via formation of dead-space microdomains. *Glia*, 62(7):1053–1065, Jul 2014.
- [35] John L. Skousen, Michael J. Bridge, and Patrick A. Tresco. A strategy to passively reduce neuroinflammation surrounding devices implanted chronically in brain tissue by manipulating device surface permeability. *Biomaterials*, 36:33–43, Jan 2015.
- [36] Eva Syková and Charles Nicholson. Diffusion in brain extracellular space. *Physiol Rev*, 88(4):1277–1340, Oct 2008.
- [37] J. N. Turner, W. Shain, D. H. Szarowski, M. Andersen, S. Martins, M. Isaacson, and H. Craighead. Cerebral astrocyte response to micro-machined silicon implants. *Exp Neurol*, 156(1):33–49, Mar 1999.
- [38] Matthew P Ward, Pooja Rajdev, Casey Ellison, and Pedro P Irazoqui. Toward a comparison of microelectrodes for acute and chronic recordings. *Brain Res*, 1282:183–200, Jul 2009.
- [39] M. Welkenhuysen. *Electrical brain stimulation and microrecording: Research in animal models of psychiatric disorders and in vivo evaluation of a neural probe*. PhD thesis, Catholic university of Leuven, KU Leuven, Leuven, 2011.

- [40] Stephen W. Wheatcraft and Mark M. Meerschaert. Fractional conservation of mass. *Advances in Water Resources*, 31(10):1377 – 1381, 2008.
- [41] Brent D Winslow, Michael B Christensen, Wen-Kuo Yang, Florian Solzbacher, and Patrick A Tresco. A comparison of the tissue response to chronically implanted parylene-c-coated and uncoated planar silicon micro-electrode arrays in rat cortex. *Biomaterials*, 31(35):9163–9172, Dec 2010.
- [42] Brent D. Winslow and Patrick A. Tresco. Quantitative analysis of the tissue response to chronically implanted microwire electrodes in rat cortex. *Biomaterials*, 31(7):1558–1567, Mar 2010.
- [43] Fanrong Xiao, Jan Hrabe, and Sabina Hrabetova. Anomalous extracellular diffusion in rat cerebellum. *Biophys J*, 108(9):2384–2395, May 2015.
- [44] Yinghui Zhong and Ravi V Bellamkonda. Dexamethasone-coated neural probes elicit attenuated inflammatory response and neuronal loss compared to uncoated neural probes. *Brain Res*, 1148:15–27, May 2007.